New Approach to Characterize Juvenile Osteochondritis Dissecans

Saba Pasha, PhD
Eileen P. Storey BA
Theodore J.Ganley MD

Department of Orthopaedic Surgery
School of Medicine
University of Pennsylvania
Philadelphia, Pennsylvania, USA

Background

Juvenile osteochondritis dissecans (JOCD) is an idiopathic condition affecting the subchondral bone and the articular cartilage in children with open growth plates. If left untreated, patients with OCD lesions can develop early onset osteoarthritis.[1,2] The incidence of OCD ranges from 18-30 cases per 100,000 in the population; however, over the past decade this number has increased particularly in young athletes due to rising awareness, more frequent use of advanced imaging, and competitive sports participation at an earlier age.[3–5] Current non-surgical treatment, including activity restriction and/or immobilization for 6 to 18 months, has been reported to be effective in only 50-67% of children with stable OCD.[3] Currently no systematic approach exists to identify those patients who can benefit from non-surgical treatment. Thus, non-operative approaches may fail after up to 18 months of activity restriction resulting in an unstable lesion that requires surgical intervention.[6–10] Since the underlying pathomechanism of this condition is unknown, effective and early intervention for successful treatment is difficult. The American Academy of Orthopedic Surgeons published a guideline to improve the diagnosis and treatment of OCD of the knee in immature and young mature patients; however,due to the nature,unknown mechanism, multifactorial etiology of the condition, and treatment variability among practicing surgeons, most of these suggestions were inconclusive.[11–13] This suggests a compelling need to further investigate the possible risk factors associated with development of OCD in young patients.

Over 50% of studies that investigated the etiology of this condition suggested trauma or repetitive movement associated with increased stress in the dominant knee.[13] However, no studies have considered if specific 3D femoro-tibia alignment and 3D range of motion are associated with development of OCD in athletes. A previously published study looked at the association between medial condyle OCD and varus axis and lateral condyle OCD and valgus axis using AP X-ray images.[14] Although this study strongly suggested an association between femoro-tibial alignment and the development of an OCD lesion, only varus/valgus 2D angles were included and 3D alignmentof the femur and tibia were not considered. Despite the years of clinical evaluation of OCD and the collective knowledge on the etiology, diagnosis, and treatment of this condition, a 3D biomechanical analysis associating 3D skeletal parameters to abnormal retropatellar or tibial spine loading and development of OCD in adolescents and young adults has not yet been performed.[13]

The emerging technology of low-dose stereoradiography system can be used to acquire biplanar X-rays and generate 3D reconstruction of the bones in an upright position.The weight-bearing position allows for analysis of the 3D alignment of the bones as patients stand. We aimed to explore the applicability of this new technology in exploring the relationship between the geometrical parameters of the lower extremities and the location of the unilateral or bilateral lesion of the knee in juvenile OCD.

The objective of this study was to characterize the 3D femoro-tibial geometrical parameters using sterEOS 2D/3D X-ray post-processing platform in a group of adolescents with stable or unstable unilateral or bilateral OCD of the knee. We hypothesized that femoral mechanical axis alignment and femoro-tibial torsion are significantly associated with the location of the OCD lesion.

Methods

Subjects

A total of three patients who presented with unilateral or bilateral OCD of the knee on their MRI were recruited for this pilot analysis. The exclusion criteria were previous surgical intervention on the knee or hip and any other neuromuscular condition. Patients had to be able to stand for 30 seconds without any external support. Patient ages ranged from 8 to 18 years. One asymptomatic age, sex-matched control was included. This pilot analysis was approved by the Institutional Review Board at the Children's Hospital of Philadelphia and consent was obtained from all participating subjects.

Clinical data collection and 3D imaging

Patients' charts and MRI were consulted to determine the location of the OCD lesion. Full biplanar X-ray images (AP and lateral) of

the lower extremities, with the pelvis included in weight-bearing standing position, were taken by the EOS stereo-radiography imaging system (EOS imaging, Paris, France). 3D reconstruction of the lower extremities was generated in SterEOS2D/3D, a validated and FDA-approved software for 3D reconstruction of the spine and lower extremities images (Figure 1A). The center of the femoral heads was determined by fitting a circle to the femoral heads in AP and lateral X-rays. Femoral and tibia condyle notches were digitized manually. A tangent line to femoral and tibial condyles was digitally traced to calculate the femur (FMA) and tibia mechanical angles (TMA) (Figure 1B). A total number of 21 2D /3D alignment and morphological parameters of the lower extremities and pelvis were measured in the cohort, including pelvic incidence, sacral slope, sagittal pelvic tilt, lateral pelvic tilt, pelvic rotation, femoral heads diameter, femoral offset, neck shaft angle, neck length, mechanical femoro-tibial angle (MFT), valgus/varus angles, flexion/extension angles, femur length, tibia length, mechanical and anatomical axes lengths, valgus/varus angles, knee flexion/extension, femoral and tibial mechanical angle, HSK angle, and axial plane parameters (tibial and femoral torsion, and femoro-tibial rotation).

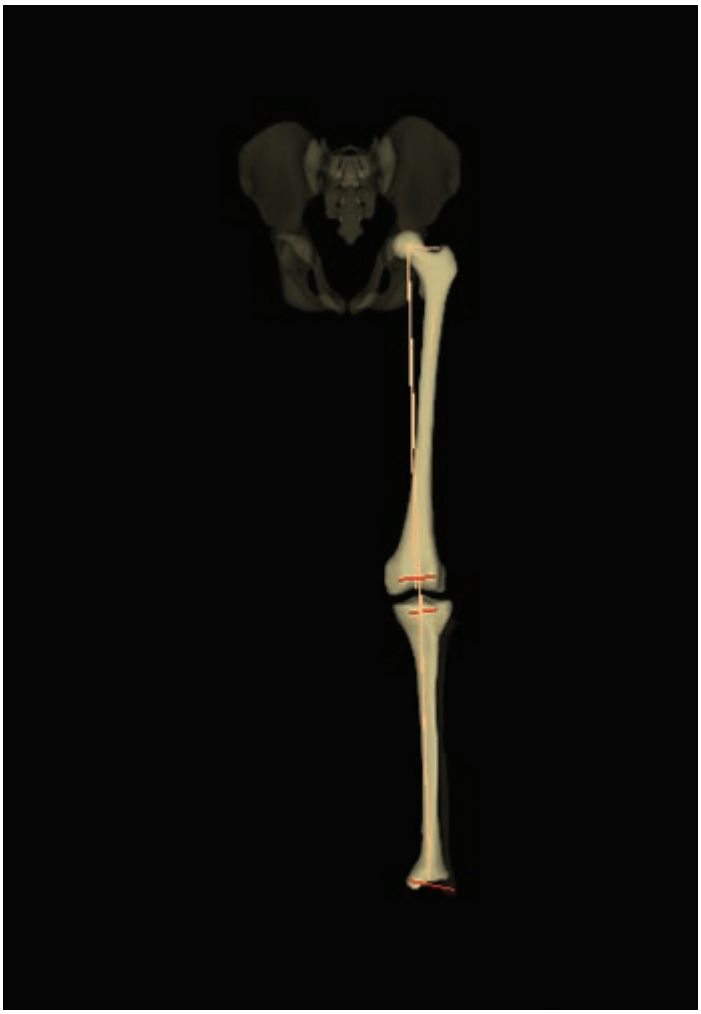

Figure 1A. EOS 3D reconstruction of a case patient's lower extremity.

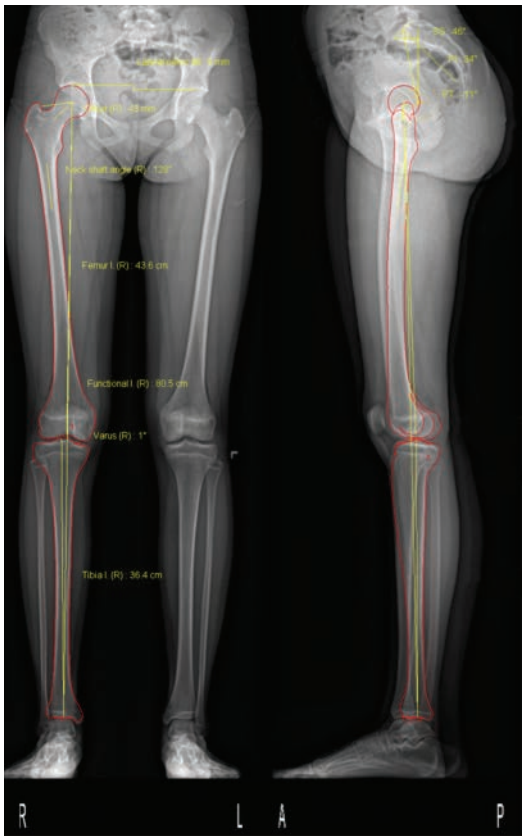

Figure 1B. Alignment and morphological parameters of the lower extremities in both AP and lateral views.

Results

One patient had left knee OCD while the other two had a lesion in their right knee. Patients' clinical data, including the demographics and the location of the lesions, are summarized in Table 1 for the three patients. The 2D and 3D measurements of the legs for the patients and control are summarized in Table 2. Higher femorotibial rotation was observed in OCD patients (10.7 versus 2.8 degrees).

Discussion

OCD is a rare disease with an unknown pathogenesis. Although multiple factors have been associated with OCD development in adolescents, the impact of the 3D alignment of the femur and tibia on the mechanical loading of the knee and development of OCD has not been investigated. We evaluated the clinical application of stereoradiography of the lower extremities in clinical assessment of OCD of the knee.

The association between varus/valgus knee angles measured on 2D X-rays and the OCD lesion has been investigated before; however, the relationship between 3D alignment of the femur and tibia, femoro-tibia torsion, and the OCD lesion has not previously been investigated.[14] Our results suggest SterEOS 2D/3D software can accurately produce the 3D geometry of the bone using EOS x-ray images.[15,16] Understanding the 3D alignment of the femur and tibia and its impact on the transferred force between the two bones is essential in

Table 1. Demographics and clinical data of case patients.

	Case 1	Case 2	Case 3
Age	9	14	14
Gender	Female	Female	Male
Laterality of OCD	Left	Right	Right
Location of lesion	Medial femoral condyle (lateral aspect)	Medial femoral condyle (lateral aspect)	Lateral femoral condyle
Treatment type	Non-surgical	Surgical	Surgical
History of OCD	No	Yes (Left)	No

Table 2. 2D and 3D leg measurements for the case patients and age-matched control.

Femur		**Case 1**	**Case 2**	**Case 3**	**Control 1**
Femoral head diameter (mm)	3D	29	44	47	34
	2D	--	--	--	--
Femoral offset (mm)	3D	31	43	34	33
	2D	--	--	--	--
Neck length (mm)	3D	38	54	51	40
	2D	39	53	44	43
Neck shaft angle (deg)	3D	127.5	127.5	139.6	125.7
	2D	125.1	128.2	137.8	122.7
Lengths					
Femur length (cm)	3D	31.9	43.6	41.0	31.8
	2D	31.9	43.5	38.7	31.6
Tibia length (cm)	3D	26.5	36.4	34.6	26.5
	2D	26.3	36.4	34.3	26.2
Functional length (cm)	3D	59.1	80.5	75.6	59.1
	2D	58.9	80.5	73.4	58.4
Anatomical length (cm)	3D	58.5	79.9	75.6	58.3
	2D	58.2	79.9	73.0	57.8
Knee					
Valgus/Varus (deg)	3D	0.4	-1.2	2.8	0.6
	2D	0.9	-1.3	3.6	0.3
Knee flexion/knee extension	3D	5.3	-2.2	11.6	0.6
(deg)	2D	5.8	-1.8	9.8	0.2
Femoral mechanical angle (deg)	3D	91.6	92.5	92.4	90.5
	2D	91.1	92.7	94.8	90.9
Tibial mechanical angle (deg)	3D	87.7	86.4	91.9	89.8
	2D	88.0	86.4	88.7	89.1
HKS (deg)	3D	4.6	4.1	3.9	3.7
	2D	4.3	3.5	3.7	4.1
Torsions					
Femoral torsion (deg)	3D	-5.9	1.1	-16.4	-4.8
	2D	--	--	--	--
Tibial torsion (deg)	3D	31.2	53.1	40.6	41.3
	2D	--	--	--	--
Femorotibial rotation (deg)	3D	12.5	-10.9	-17.0	-2.8
	2D	--	--	--	--

characterizing the underlying biomechanical parameters associated with OCD progression and development.

The stereoradiography system, EOS™ imaging, also reduces the radiation dose 3 to 4 times compared to the scanograms performed with computed radiography (CR) while conserving X-ray images' quality. The reliability of this imaging modality has been tested in identifying the lower limb torsion and length discrepancy.[15,16] While application of the stereoradiography imaging in OCD clinical evaluation reduces the radiation exposure and examination time significantly, the reliability of this new technology in clinically evaluating OCD of the knee has not been investigated.

This study demonstrates the applicability of low-dose stereoradiography of OCD of the knee. The 3D parameters can improve the classification of OCD of the knee and highlight the mechanical factors associated with OCD development. This novel approach has potential to improve understanding of the underlying pathomechanism associated with OCD of the knee.

Conclusion

The applicability of the stereoradiography imaging in 3D evaluation of OCD of the knee was investigated. This technique can reduce the radiation dose while providing quantitative information regarding the mechanical factors associated with OCD development.

References

1. Shea KG, Jacobs JCJ, Carey JL, Anderson AF, Oxford JT. Osteochondritis dissecans knee histology studies have variable findings and theories of etiology. *Clin Orthop Relat Res.* United States; 2013 Apr;471(4):1127–36.

2. Ganley, TJ; Flynn J. Osteochondritis dissecans. In: WN S, editor. *Insall & Scott Surgery of the Knee.* 4th ed. Philadelphia: Elsevier; 2006. p. 1234–41.

3. Hughston JC, Hergenroeder PT, Courtenay BG. Osteochondritis dissecans of the femoral condyles. *J Bone Joint Surg Am.* United States; 1984 Dec;66(9):1340–8.

4. Linden B. The incidence of osteochondritis dissecans in the condyles of the femur. *Acta Orthop Scand.* Denmark; 1976 Dec;47(6):664–7.

5. Kessler JI, Nikizad H, Shea KG, Jacobs JCJ, Bebchuk JD, Weiss JM. The demographics and epidemiology of osteochondritis dissecans of the knee in children and adolescents. *Am J Sports Med.* United States; 2014 Feb;42(2):320–6.

6. Crawford DC, Safran MR. Osteochondritis dissecans of the knee. *J Am Acad Orthop Surg.* United States; 2006 Feb;14(2):90–100.

7. Cahill BR, Phillips MR, Navarro R. The results of conservative management of juvenile osteochondritis dissecans using joint scintigraphy. A prospective study. Am J Sports Med. United States; 1989;17(5):601–6.

8. Cepero S, Ullot R, Sastre S. Osteochondritis of the femoral condyles in children and adolescents: our experience over the last 28 years. *J Pediatr Orthop B.* United States; 2005 Jan;14(1):24–9.

9. Pill SG, Ganley TJ, Milam RA, Lou JE, Meyer JS, Flynn JM. Role of magnetic resonance imaging and clinical criteria in predicting successful nonoperative treatment of osteochondritis dissecans in children. *J Pediatr Orthop.* United States; 2003;23(1):102–8.

10. Wall E, Von Stein D. Juvenile osteochondritis dissecans. *Orthop Clin North Am.* United States; 2003 Jul;34(3):341–53.

11. Chambers HG, Shea KG, Anderson AF, Jojo Brunelle TJ, Carey JL, Ganley TJ, et al. American Academy of Orthopaedic Surgeons clinical practice guideline on: the diagnosis and treatment of osteochondritis dissecans. *J Bone Joint Surg Am.* United States; 2012 Jul;94(14):1322–4.

12. Ganley, TJ; Gaugler RL; Kocher MS FJJK. Osteochondritis dissecans of the knee. *Oper Tech Sports Med.* 2006;14(3):147–58.

13. Edmonds EW, Polousky J. A review of knowledge in osteochondritis dissecans: 123 years of minimal evolution from Konig to the ROCK study group. *Clin Orthop Relat Res.* United States; 2013 Apr;471(4):1118–26.

14. Jacobi M, Wahl P, Bouaicha S, Jakob RP, Gautier E. Association between mechanical axis of the leg and osteochondritis dissecans of the knee: radiographic study on 103 knees. *Am J Sports Med.* United States; 2010 Jul;38(7):1425–8.

15. Schlatterer B, Suedhoff I, Bonnet X, Catonne Y, Maestro M, Skalli W. Skeletal landmarks for TKR implantations: evaluation of their accuracy using EOS imaging acquisition system. Orthop *Traumatol Surg Res.* France; 2009 Feb;95(1):2–11.

16. Escott BG, Ravi B, Weathermon AC, Acharya J, Gordon CL, Babyn PS, et al. EOS low-dose radiography: a reliable and accurate upright assessment of lower-limb lengths. *J Bone Joint Surg Am.* United States; 2013 Dec;95(23):e1831–7.